

# Experimental Determination of Continuous Phase Overall Mass Transfer Coefficients Case Study: Kühni Extraction Column

*Asadollahzadeh, Mehdi\**<sup>+</sup>

*Department of Chemical Engineering, Iran University of Science and Technology (IUST),  
P.O. Box 16765-163 Tehran, I.R. IRAN*

*Torkaman, Rezvan; Torab-Mostaedi, Meisam*

*Materials and Nuclear Fuel Research School, Nuclear Science and Technology Research Institute,  
P.O. Box 11365-8486 Tehran, I.R. IRAN*

**ABSTRACT:** *Experimental data obtained in a pilot-scale Kühni liquid-liquid extraction column were used to obtain. In this study, volumetric overall mass transfer coefficients were measured and correlated under different operating variables in a 113 mm diameter Kühni column. Both mass transfer directions are considered in the experiments. The effect of operating parameters on the volumetric overall mass transfer coefficients has been investigated. According to obtained results, mass transfer performance is strongly dependent on rotor speed and mass transfer direction, although only slightly dependent on phase flow rates. A novel empirical correlation is developed for prediction of overall continuous phase Sherwood number based on dispersed phase holdup, Reynolds number and mass transfer direction. The proposed correlations based on dimensionless numbers can be considered as a useful tool for the possible scale up of the Kühni column.*

**KEYWORDS:** *Kühni column; Overall mass transfer coefficients; Mass transfer direction; Sherwood number.*

## INTRODUCTION

Liquid-liquid extraction or solvent extraction is a separation process which is based on the different distribution of the components to be separated between two liquid phases. It depends on the mass transfer of the component to be extracted from a first liquid phase to a second one [1, 2].

Different types of liquid-liquid columns are in use nowadays, which can be classified into two main

categories: agitated (RDC, ORC & Kühni) and pulsed (packed, sieve plate & disc and doughnut) columns [3-6].

The Kühni contactor represents a logical development of the RDC and ORC columns, in which the baffled impellers of the latter are replaced by the unbaffled double entry turbines, and the annular partition plates between stages in the former are replaced by the perforated stator plates [7].

---

\* To whom correspondence should be addressed.

+ E-mail: mehdiasadollahzadeh@alumni.iust.ac.ir

1021-9986/2017/5/149-161

13/\$/6.30

In most industrial extraction equipment, one phase is dispersed as a swarm in a second continuous phase. This method of contact has the advantage of providing a large interfacial area per unit volume for the mass transfer [8, 9].

The design and scale up of an extractor needs the calculation of two independent parameters including the cross-sectional area and the height of the column. The first one is required to accommodate the desired flows without flooding and the second one should be determined to reach the appropriate performance of extraction columns [10].

Therefore, knowledge of mass transfer performance is of fundamental importance for the design and development of practical extraction columns. Mixing is often applied to the extraction columns such as RDC, Kühni, and ORC columns in order to improve the phase contact. The performance of the apparatus is often ameliorated by the use of impellers. The agitation modifies the apparatus hydrodynamics by inducing turbulence in the flow thus improving the interphase contact and intensifying the mass transfer [11, 12].

The knowledge of axial mixing in extraction column is necessary for understanding the fundamental processes involved in the mass transfer. Failure to account for axial mixing may lead to large errors in column dimensions. It has been reported that axial dispersion in extraction columns lowers the process efficiency as much as 30% [13].

Use axial mixing or backflow model for design and scale-up is now developed for determination of height of extraction column. In this method, one parameter is considered for all deviations from the ideal plug flow conditions [14].

The investigation has been focused to study the axial dispersion in continuous phase of liquid–liquid extraction columns such as spray towers [15-17], reciprocating plate extraction columns [18, 19] and pulsed sieve plate extraction columns [20, 21]. Although, a few studies can be found in which this effect has been taken into account.

Determining mass transfer coefficient in an extractor is difficult due to significant uncertainty. Although, the Kühni was applied appropriately for a number of separation processes, limited experimental data are available from the literature on the mass transfer performance of Kühni extraction columns.

This research work examines the ability of an axial dispersion model with correlations to predict the

performance of a Kühni column. New correlations are proposed to describe the effects of agitation conditions, phase velocities, physical properties of the liquid-liquid system on the overall mass transfer coefficients.

## EXPERIMENTAL SECTION

### *Description of the Equipment*

A pilot scale unit of Kühni extraction column was constructed. Internal diameter of Kühni contactor is 113 mm and it has 10 stages. Agitation at each stage is achieved with 50 mm diameter shrouded six-blade turbine agitator with an accurate speed control. The interface location of the two phases at the top of the heavy-phase inlet and under the light-phase outlet in the upper settler was automatically controlled by an optical sensor. A solenoid valve (a normally closed type) was provided at the outlet stream of the heavy phase. When the interface location was meant to change, the optical sensor sent a signal to the solenoid valve and the heavy phase was allowed to leave the column by opening the diaphragm of the solenoid valve. The light phase was allowed to leave the column via an overflow. A schematic diagram of the experimental apparatus is shown in Fig. 1. The geometrical data of the investigated extraction column are given in Table 1.

### *Materials Used*

All experiments were conducted at ambient temperature, using a liquid–liquid system according to the recommendations of the European Federation of Chemical Engineering [22]. The system was toluene–acetone–water. The experiments were carried out in both mass transfer directions. In all of the experiments, dilute solutions were investigated with approximately 3.5 wt% acetone as transferred solute in the organic or aqueous phase.

The physical properties of these systems are listed in Table 2. Technical-grade solvents of at least 99.5 wt% purity were used as the dispersed phase and distilled water was used as the continuous phase.

### *Analytic Procedure*

In each experiment the following variables were measured:

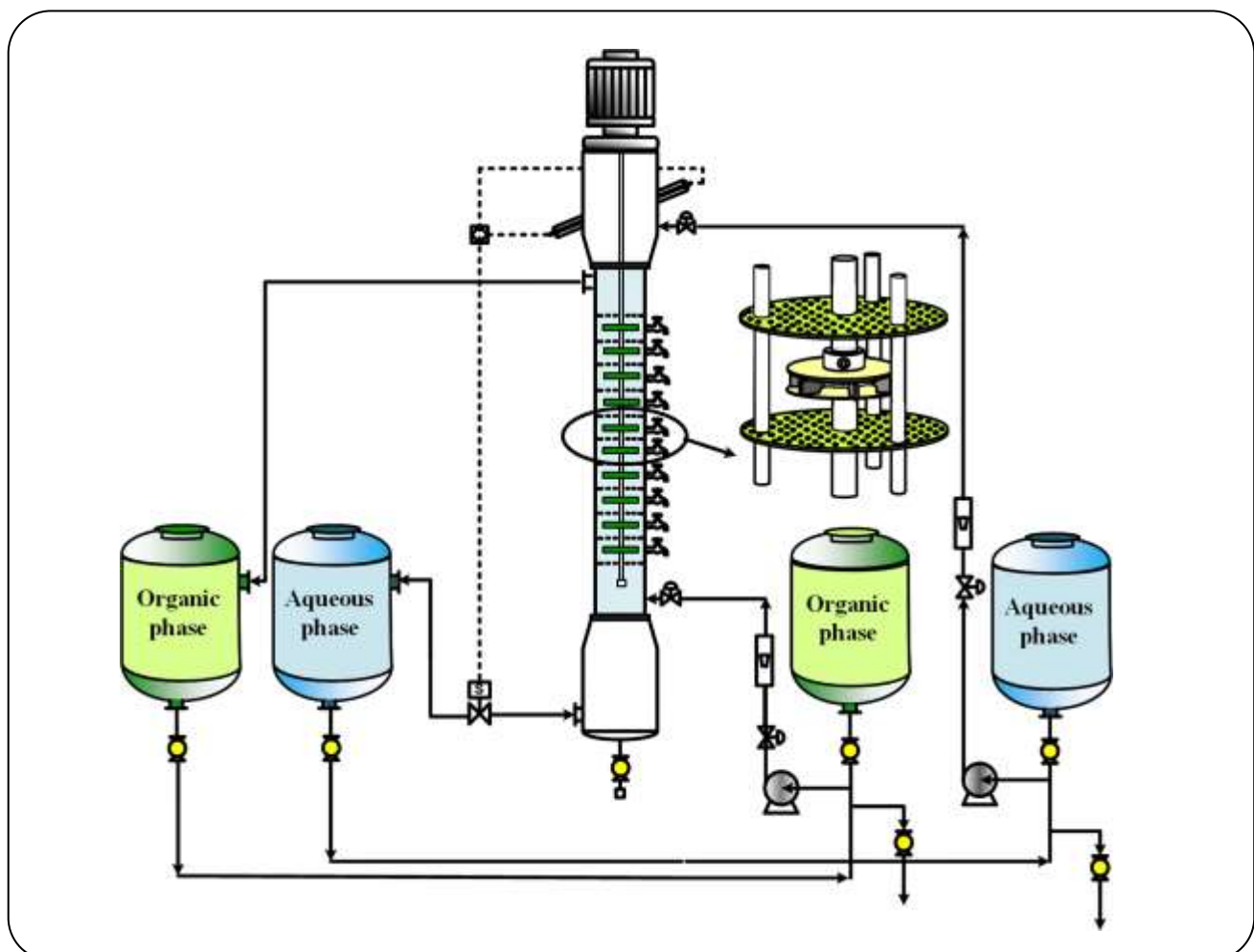
(1) Before starting each run, the aqueous and organic phases were first mutually saturated, after which acetone

**Table 1: The geometrical data of the investigated extraction column.**

Column diameter (m)	0.117
Shrouded six-bladed turbine diameter (m)	0.05
Column working height (m)	0.7
Stator plate fractional free area	0.212
No. of compartments (-)	10

**Table 2: Physical properties of liquid systems at 20 °C [22].**

Physical property	Toluene/acetone/water
$\rho_c$ [kg/m <sup>3</sup> ]	994.4-995.7
$\rho_d$ [kg/m <sup>3</sup> ]	864.4-865.2
$\mu_c$ [mPa.s]	1.059-1.075
$\mu_d$ [mPa.s]	0.574-0.584
$\sigma$ [mN/m]	27.5-30.1
$D_c$ [m <sup>2</sup> /s]	$1.09-1.14 \times 10^{-9}$
$D_d$ [m <sup>2</sup> /s]	$2.7-2.8 \times 10^{-9}$

**Fig. 1: A schematic diagram of the experimental apparatus.**

was added to the dispersed (organic) phase to give a concentration of about 3.5 wt% acetone.

(2) Samples of each phase were taken at their inlets to the column and used for determination of the initial solute concentration.

(3) The rotor speed and the continuous phase flow rate were set at the desired valves and the dispersed phase gradually admitted into the column up to the desired volumetric flow rate.

(4) The interface location was then maintained at the desired height, and the system was allowed to reach steady-state.

(5) For all experiments, the steady-state condition could be achieved after three times the residence times.

(6) At the end of each run, samples of the aqueous and organic phases were taken at their respective outlet.

(7) The solute concentrations were then determined by UV-visible spectroscopy.

(8) Dispersed phase holdup ( $\phi$ ) along the column using shutdown procedure, when the operation became steady state, the dispersed phase and continuous phase inlet and outlet valves were quickly closed. The dispersed phase was allowed to settle and the difference in the interface level location was used to measure the total holdup. The holdup was defined as the ratio of the displaced dispersed phase volume to the total volume of the extraction region.

(9) Sauter mean diameter of droplets ( $d_{32}$ ), in the way that pictures of four different heights of the column have been captured in each experiment by means of a very high-resolution Nikon D5000 camera and have been compared with the stators thickness served as the reference for the drop size measurements. The Sauter mean diameter was calculated from the following equation:

$$d_{32} = \frac{\sum_{i=1}^N n_i d_i^3}{\sum_{i=1}^N n_i d_i^2} \quad (1)$$

where  $n_i$  denotes the number of drops of diameter  $d_i$ .

The specific interfacial area was obtained by the following equation:

$$a = \frac{6\phi}{d_{32}} \quad (2)$$

All experiments were performed far from flooding conditions. For each liquid-liquid system the operating variables were systematically varied to determine their influence on the volumetric overall mass transfer coefficient.

#### Model for mass transfer coefficient

According to the axial diffusion model and material balance in the extraction column, over the differential elements of the extraction column with a total effective height,  $H$ , the equation set for steady state process is established using following equation, under the constant superficial velocities  $V_c$  and  $V_d$  at any given agitation rate [8]:

$$\frac{\partial}{\partial Z} \left( x - \frac{1}{P_c} \frac{\partial x}{\partial Z} \right) + N_{oc} (x - x^*) = 0 \quad (3)$$

$$\frac{\partial}{\partial Z} \left( y + \frac{1}{P_d} \frac{\partial y}{\partial Z} \right) + N_{oc} \frac{V_c}{V_d} (x - x^*) = 0 \quad (4)$$

It should be noted that in Eqs. (3) and (4)  $N_{oc} = K_{oc} a H / V_c$  represents  $(NTU)_{oc} = H / (HTU)_{oc}$ .  $Pe_c$  and  $Pe_d$  are Peclet numbers and may be represent as Eqs. (5) and (6):

$$Pe_c = \frac{H V_c}{E_c} \quad (5)$$

$$Pe_d = \frac{H V_d}{E_d} \quad (6)$$

The axial mixing in the dispersed phase is generally less pronounced than that in the continuous phase. In the present work, dispersed phase axial dispersion is assumed to be negligible. The following boundary conditions can be used for the extraction column:

$$\frac{d\chi}{dZ} = 0, \quad (7)$$

$$dy = y^\circ \text{ (at the bottom of the extractor), } Z=1$$

$$-\frac{d\chi}{dZ} = Pe_\chi (\chi^\circ - \chi), \quad (8)$$

$$\text{(at the top of the extractor), } Z=0$$

By using the continuous phase axial dispersion coefficient, the measured dispersed and continuous phase

concentrations, together with the equilibrium data, and the boundary conditions, the experimental values of volumetric overall mass transfer coefficients are calculated from Eqs. (3) and (4).

In the current study, dispersed phase axial dispersion is taken to be negligible, with the continuous phase axial mixing coefficient calculated by the following equation given by *Kumar and Hartland* [23]:

$$\frac{E_c}{\bar{V}_c h_c} = 0.42 + 0.29 \left( \frac{V_d}{V_c} \right) + \quad (9)$$

$$\left[ 1.05 \times 10^{-2} \left( \frac{ND_R}{V_c} \right) + \frac{13.38}{3.18 + \left( \frac{ND_R}{V_c} \right)} \right] \times \left( \frac{V_c D_R \rho_c}{\eta_c} \right)^{-0.08} \left( \frac{D_c}{D_R} \right)^{0.16} \left( \frac{D_c}{h_c} \right)^{0.1} e$$

## RESULTS AND DISCUSSION

The influence of agitation rate on the volumetric overall mass transfer coefficient, mean drop size and holdup are shown in Fig. 2 (a, b and c). and the pictures of drop sizes for dispersed to continuous transfer with different rotor speed are shown in Fig 3.

As expected, a higher rotor speed leads to a lower value of the mean drop size and a higher value of the holdup. The interfacial area for mass transfer increases with both effects. However, the reduction of drop diameter results in a reduction of the overall mass transfer coefficient due to the reduction of internal circulations inside the drop. The experimental findings indicate that the effect of the interfacial area is larger than that of the overall mass transfer coefficient and, consequently, the mass transfer performance increases with an increase in rotor speed.

Fig. 2 also reveals that the extraction column performance changes with the mass transfer direction. When the mass transfer carries out from the continuous to the dispersed phase, acetone concentration in the top of drop is lower than the bottom of the drop. This interfacial tension driving force results in interface moves in opposition to the direction of the inner circulation generated in the droplet. So, interface deformation can be happened when the direction of mass transfer is  $c \rightarrow d$ . Drop deformation such as the break-up process leads

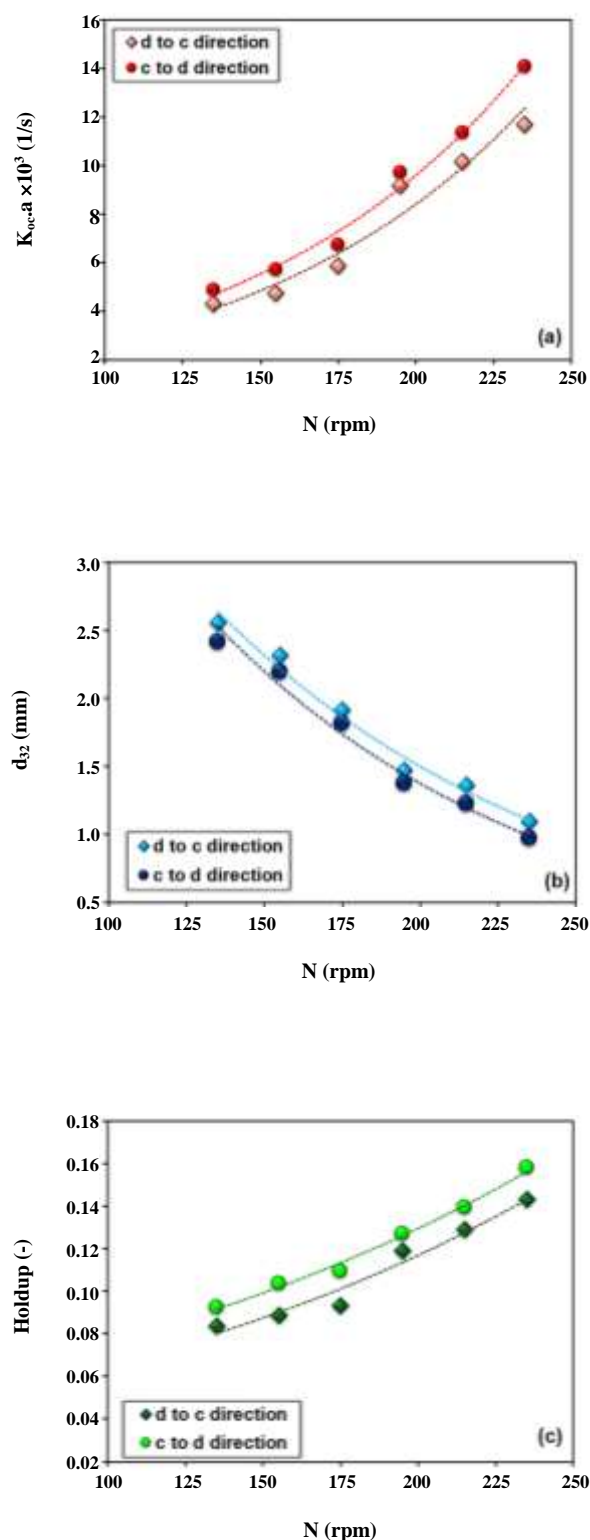


Fig. 2: Effect of agitation rate on (a) Volumetric overall mass transfer (b) Sauter mean drop diameter and (c) Holdup ( $V_c = V_d = 0.62$  mm/s).

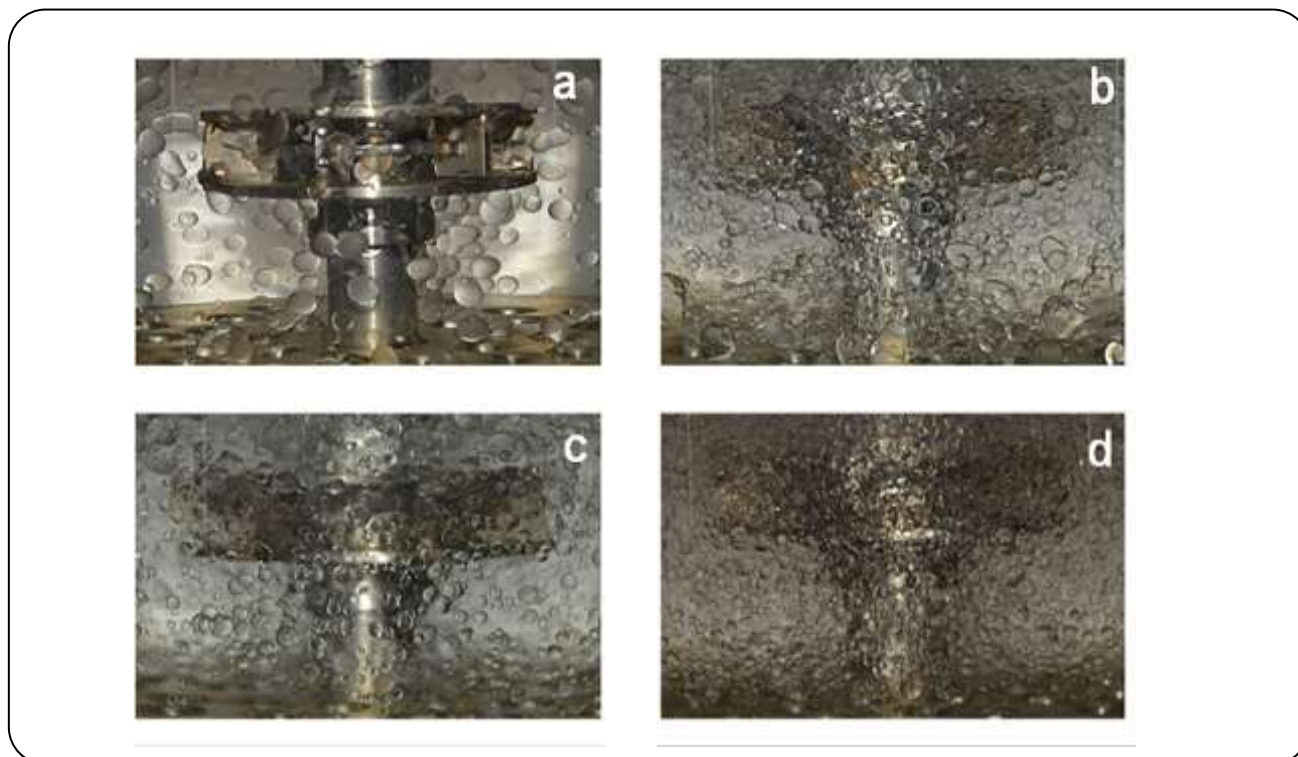


Fig. 3: Pictures of drop sizes with different rotor speeds for dispersed to continuous transfer (a) 135, (b) 175, (c) 195, (d) 235 rpm.

to the enhancement of mass transfer. For  $d \rightarrow c$  mass transfer, the interfacial tension driving force is opposite. The interface motion and the inner circulation are in the same direction. Consequently, the droplets can be more stable than in the  $c \rightarrow d$  direction. Therefore, drops tend to be smaller in  $c \rightarrow d$  mass transfer than opposite direction (see Fig. 2 (b)). In addition, the dispersed phase holdup is larger for  $c \rightarrow d$  acetone transfer because of the smaller droplets formation (see Fig. 2 (c)). Finally, in the case of  $c \rightarrow d$  direction, the interfacial area is higher than that of in the  $d \rightarrow c$  because of the lower drop size and higher holdup.

The higher mass transfer coefficient in the  $d \rightarrow c$  direction than  $c \rightarrow d$  direction for acetone transfer can be explained via the interfacial turbulence induction of local differences in the acetone concentration. The interfacial tension driving force is occurred due to interfacial movement and internal circulation generated in the drop. The latter mentioned phenomena are in the same direction in  $c \rightarrow d$  acetone transfer, while in  $d \rightarrow c$  acetone transfer, they are in the opposing directions. For mentioned reason, internal agitation within the drop would carries out in  $d \rightarrow c$  transfer systems which results in higher mass transfer

coefficient than that realized for  $c \rightarrow d$  transfer systems. It is seen that the influence of interfacial area on the mass transfer performance of extraction column is lower than that of the overall mass transfer coefficient.

The influence of continuous phase velocity on volumetric overall mass transfer coefficient, mean drop size and holdup are shown in Fig. 4 (a, b and c). It can be seen that the volumetric overall mass transfer coefficient and interfacial area increase with an increase in continuous phase velocity in the range of velocities studied.

The dispersed phase holdup increases with the increase in continuous phase velocity due to a reduction of the relative velocity between the drops and continuous phase. Moreover, this effect is not appreciable on the size of the dispersed drops (Fig.4b). Therefore, the interfacial area increases with the increase in holdup. The overall mass transfer coefficient increases with  $V_c$  due to an increase in drag forces arising from the relative velocity between a drop and the continuous phase. Consequently, the mass transfer performance increases with the increase in the interfacial area and overall mass transfer coefficient.

It is also observed that the overall mass transfer coefficient slightly increases with an increase in the

continuous phase velocity. Therefore, the column performance increases with the both effects.

Fig. 5 (a, b and c) shows the influence of dispersed phase velocity on volumetric overall mass transfer coefficient, mean drop size and holdup respectively. As it can be seen from Figs. 5(b) and (c), the Sauter mean drop diameter and dispersed phase holdup increase with the enhancement of dispersed phase velocity in the  $c \rightarrow d$  and  $d \rightarrow c$  mass transfer directions, although, the influence of the dispersed phase holdup on the interfacial area is dominant than that of the mean drop size. Thus, there is an increase in the interfacial area with increasing of dispersed phase velocity. As it is also seen, the overall mass transfer coefficient increases with the enhancement of the dispersed phase velocity for  $d \rightarrow c$  and  $c \rightarrow d$  direction. For both mass transfer directions, the mass transfer performance in the extraction column would enhance with an increase in both overall mass transfer coefficient and the interfacial area.

Several studies have reported that mass transfer is an important parameter in liquid–liquid columns and has to be taken into account to design industrial columns. Mass transfer in the continuous phase is commonly changed by a combination of molecular diffusion, and natural or forced convection within the drop [24].

A number of empirical equations to predict mass transfer in a single drop and different types of extraction columns are available. Table 3 briefly gives a list of the published related correlations.

Table 4 is provided for comparison of experimental results of overall mass transfer coefficient with the results of previous studies. Average Absolute Relative Error (AARE) is used to determine the accuracy of current work. According to the Table 4, it can be resulted that none of the previous correlations are suitable for determination of mass transfer coefficient in the perforated rotating disc contactor.

The calculated values of the overall mass transfer coefficients ( $K_{oc}$ ) are then compared with those provided from single-drop correlations (Eqs. (10) to (17) in Table 1). This is affected by using one of the following expressions relating the overall to individual mass transfer coefficients:

$$\frac{1}{k_{oc}} = \frac{1}{k_c} + \frac{1}{mk_d} \quad (23)$$

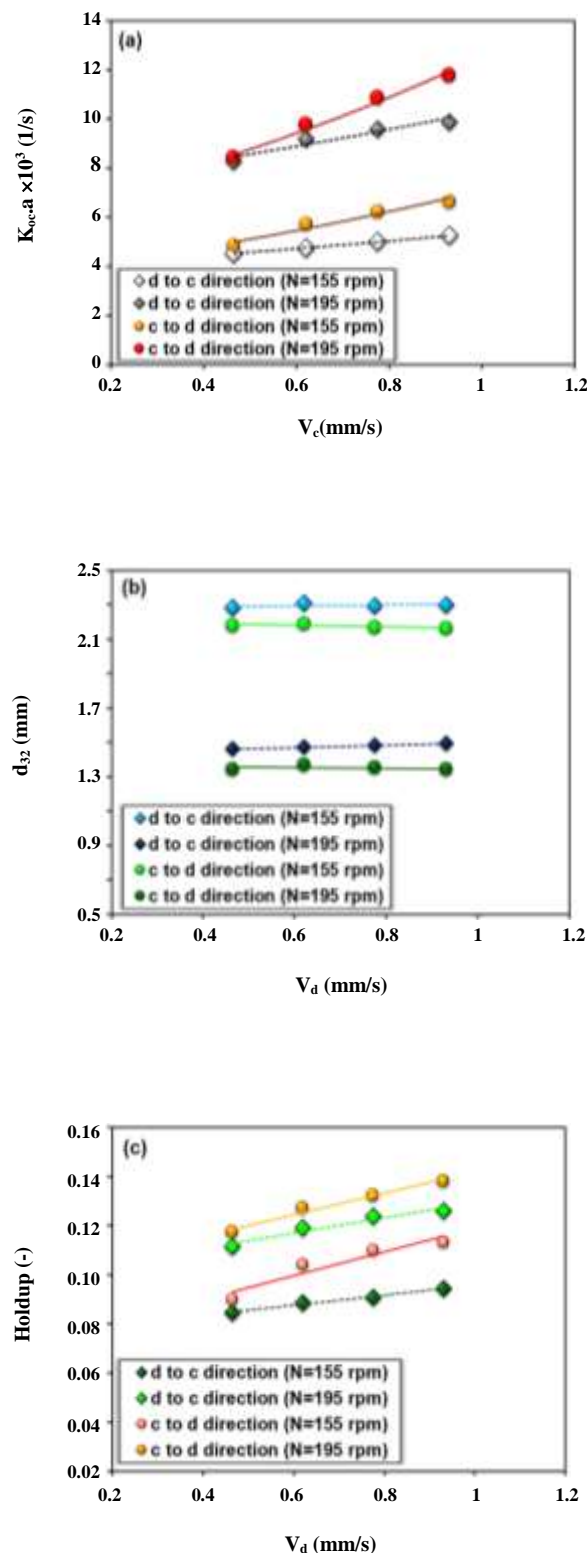


Fig. 4: Effect of continuous phase velocity on (a) Volumetric overall mass transfer the (b) Sauter mean drop diameter and (c) Hold-up ( $V_a = 0.62$  mm/s).

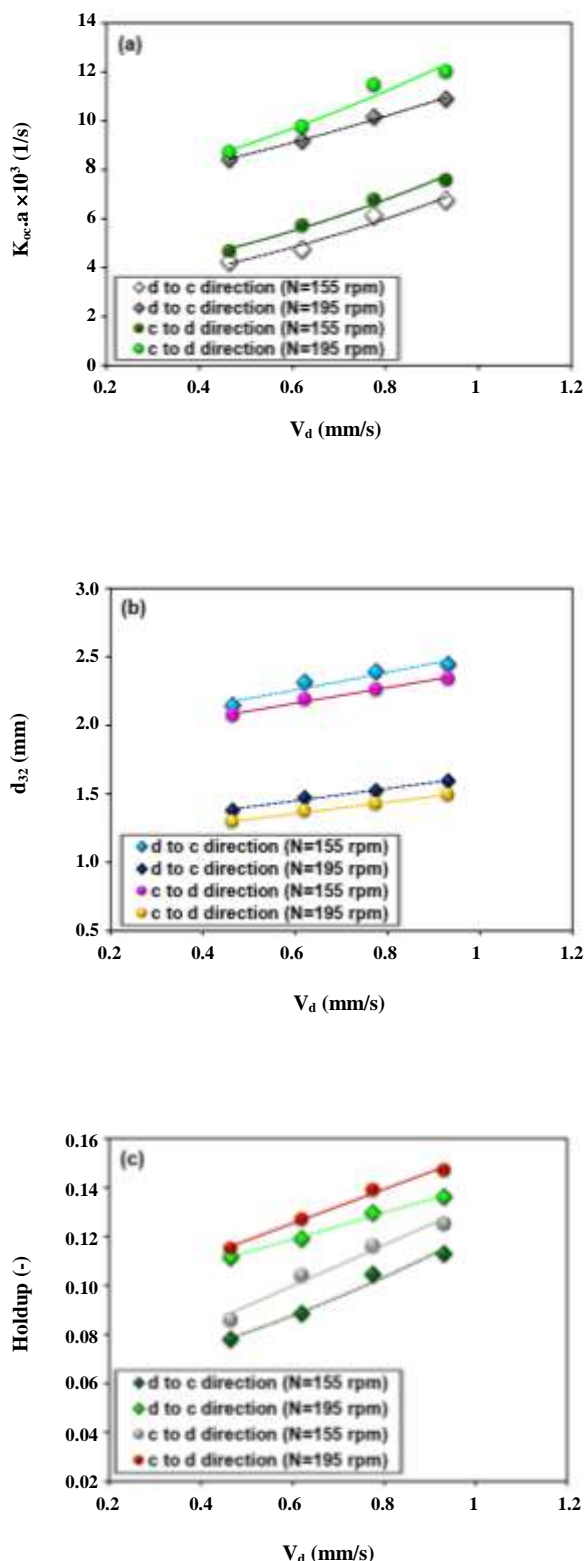


Fig. 5: Effect of dispersed phase velocity on (a) Volumetric overall mass transfer (b) Sauter mean drop diameter and (c) Hold-up ( $V_c = 0.62$  mm/s).

The Gröber equation (Eq. (24)) [36] concerns rigid drops which do not have any internal circulation and where mass transfer is more controlled by a transient molecular diffusion.

$$K_{od} = -\frac{d}{6t} \ln \left[ 6 \sum_{n=1}^{\infty} B_n \exp \left( -\frac{4\lambda_n^2 D_d t}{d^2} \right) \right] \quad (24)$$

The Kronig-Brink model (Eq. (25)) [37] assumes a laminar diffusion with an inner circulation inside the drop, induced by its relative motion, with respect to the continuous phase.

$$K_{od} = -\frac{d}{6t} \ln \left[ \frac{3}{8} \sum_{n=1}^{\infty} B_n^2 \exp \left( -\frac{64\lambda_n D_d t}{d^2} \right) \right] \quad (25)$$

The Handlos-Baron model (Eq. (26)) [38] deals with the case of drops with internal turbulent circulation and where mass transfer is controlled by turbulent diffusion.

$$K_{od} = -\frac{d}{6t} \ln \left[ 6 \sum_{n=1}^{\infty} B_n^2 \exp \left( -\frac{\lambda_n V_t t}{128d(1+\kappa)} \right) \right] \quad (26)$$

Although mass transfer into or out of drops have been investigated for many years, it is still not fully understood, since it depends on several factors. These factors include the fact that the dispersed phase mass transfer coefficient depends upon the nature, size and behavior of the drop. The presently available equations for calculation of the dispersed phase mass transfer coefficient are not usually valid over a range of drop sizes and behavior in a typical extraction column. The above equation is used for calculation of  $k_d$  for circulating drop (Eqs. (14) to (17)).

The values of error in the correlations related to these columns are rather unsatisfactory for a Kühni column. A comparison between these correlations and the experimental data is shown in Fig. 6.

In the present study, the possibility of using these correlations for prediction of overall continuous mass transfer coefficient.

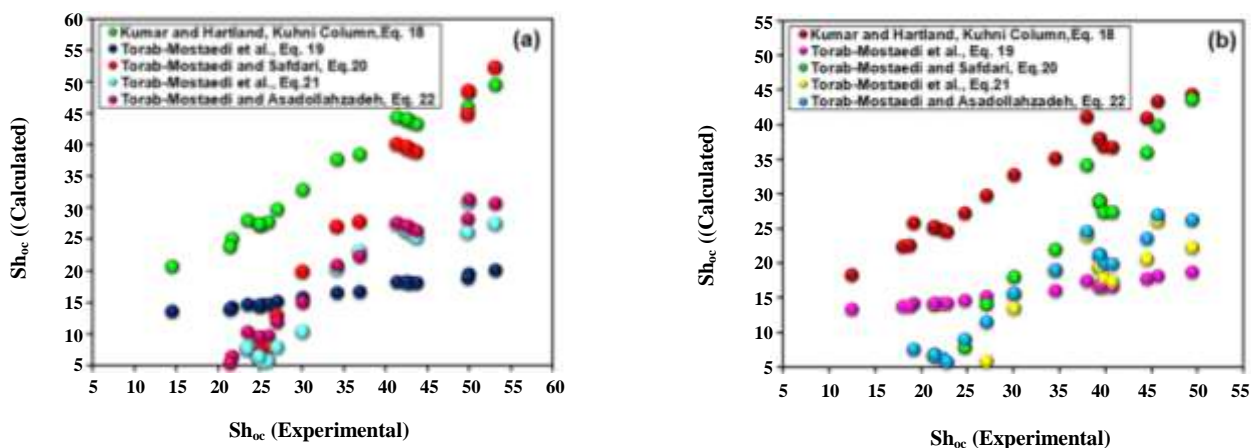
The predictive correlation for mass transfer coefficient in conjunction with holdup, drop size and physical properties are proposed to predict the performance of the columns as expressed by the following equations:

Table 3: Previous correlations for estimation of mass transfer coefficient in single drop systems and extraction columns.

Reference	Correlations
Stagnant Drops	
Lochiel and Calderbank [25]	$Sh_c = 0.7 Re^{1/2} Sc_c^{1/3}$ high Reynolds numbers (10)
Brauer [26]	$Sh_c = 2 + \left[ \frac{0.66}{1 + Sc_c} + \frac{Sc_c}{2.4 + Sc_c} \left( \frac{0.79}{Sc_c^{1/6}} \right) \right] \frac{Pe_c^{1.7}}{1 + Pe_c^{1.2}}$ $1 < Re < 100$ (11)
Skelland [24]	$Sh_c = 2 + C_1 Re^{1/2} Sc_c^{1/3}$ (12)
Clift et al. [27]	$Sh_c = 1 + 0.724 Re^{0.48} Sc_c^{1/3}$ (13)
Circulating Drops	
Garner et al. [28]	$Sh_c = -126 + 1.8 Re^{0.5} Sc_c^{0.42}$ $8 < Re < 800$ (14)
Brauer [26]	$Sh_c = 2 + 0.0511 Re^{0.724} Sc_c^{0.7}$ $4 < Re < 1000$ $130 < Sc_c < 23600$ (15)
Weber [29]	$Sh_c = 2 \left( \frac{Pe_c}{\pi} \right)^{1/2} \left[ 1 - \frac{1}{Re^{1/2}} (2.89 + 2.15 \kappa^{0.64}) \right]^{1/2}$ $\kappa \leq 2$ and $\rho_d / \rho_c \leq 4$ (16)
Steiner [30]	$\frac{Sh_c - Sh_{c,rigid}}{Sh_{c,circ} - Sh_{c,rigid}} = 1 - \exp[-4.18 \times 10^{-3} Pe_c^{0.42}]$ $10 < Re < 1200$ $190 < Sc_c < 241000$ (17) $Sh_{c,rigid} = 2.43 + 0.775 Re^{1/2} Sc_c^{1/3} + 0.0103 Re Sc_c^{1/3}$
Extraction Columns	
Kumar and Hartland [31]	$\frac{\frac{Sh_c}{1-\varphi} - Sh_{c,rigid}}{Sh_{c,\infty} - Sh_c / (1-\varphi)} = 5.26 \times 10^{-2} Re^{1/2 + 6.59 \times 10^{-2} Re^{1/4} \times Sc_c^{1/3} \left( \frac{V_s \mu_c}{\sigma} \right)^{1/3}} \frac{1}{1 + \kappa^{1.1}} \times \left[ 1 + C_1 \left\{ \frac{\psi}{g} \left( \frac{\rho_c}{g\sigma} \right)^{1/4} \right\}^{1/3} \right]$ (18) $C_1 = 4.33, 2.44, 7.5$ and $0$ for Pulsed, Karr, Kühni and Rotating Disc Column, respectively.
Torab-Mostaedi et al. [32]	$Sh_{oc} = 12.34 + 0.116 Re^{1.389}$ $Re > 10$ (19) $Sh_{oc} = 2.586 + 0.000217 Re^{4.86}$ $Re < 10$ Hanson Mixer Settler
Torab-Mostaedi and Safdari [33]	$Sh_{oc} = -49.76 + 14.8 Re^{0.64}$ $10 < Re < 150$ (d to c) (20) $Sh_{oc} = -59.35 + 27.27 Re^{0.45}$ $9 < Re < 105$ (c to d) Pulsed Packed Extraction Column
Torab-Mostaedi et al. [34]	$Sh_{oc} = -121.56 + 103.62 Re^{0.16} (1-\varphi)$ $11.73 < Re < 69.43$ (d to c) $Sh_{oc} = -119.50 + 113.30 Re^{0.12} (1-\varphi)$ $9.45 < Re < 57.08$ (c to d) pulsed Disk and Doughnut Extraction Column (21)
Torab-Mostaedi and Asadollahzadeh [35]	$Sh_{oc} = -37.31 + 22.94 Re^{0.4} (1-\varphi)$ (d to c) $Sh_{oc} = -120.72 + 117.01 Re^{0.12} (1-\varphi)$ (c to d) ARDC Extraction Column (22)

**Table 4: The values of AARE in the predicted values of Overall Sherwood number obtained by previous correlations.**

Equation	Averaged absolute values of the relative error (AARE)	
	d to c direct	c to d direct
$Sh_c$ (Lochiel and Calderbank, Eq.10) and $k_d$ (Newman, Eq.24)	78.4%	76.7%
$Sh_c$ (Brauer, Eq.11) and $k_d$ (Newman, Eq.24)	77.1%	75.2%
$Sh_c$ (Skelland, Eq.12) and $k_d$ (Newman, Eq.24)	77.8%	76.0%
$Sh_c$ (Clift et al., Eq.13) and $k_d$ (Newman, Eq.24)	77.9%	76.0%
$Sh_c$ (Garner et al., Eq.14) and $k_d$ (Kronig and Brink, Eq.25)	144.2%	124.5%
$Sh_c$ (Brauer, Eq.15) and $k_d$ (Kronig and Brink, Eq.25)	59.4%	56.8%
$Sh_c$ (Weber, Eq.16) and $k_d$ (Kronig and Brink, Eq.25)	39.4%	34.9%
$Sh_c$ (Steiner, Eq.17) and $k_d$ (Kronig and Brink, Eq.25)	57.1%	54.0%
$Sh_{oc}$ (Kumar and Hartland, RDC Column, Eq. 18)	18.9%	12.6%
$Sh_{oc}$ (Kumar and Hartland, Kühni Column, Eq. 18)	19.0%	12.7%
$Sh_{oc}$ (Torab-Mostaedi et al., Eq. 19)	48.3%	44.5%
$Sh_{oc}$ (Torab-Mostaedi and Safdari, Eq.20)	61.8%	75.9%
$Sh_{oc}$ (Torab-Mostaedi et al., Eq.21)	52.2%	60.7%
$Sh_{oc}$ (Torab-Mostaedi and Asadollahzadeh, Eq. 22)	52.5%	60.3%

**Fig. 6: Comparison of the values calculated previous models with experimental results (a) d to c direction and (b) c to d direction.**

$$Sh_{oc} = 4.89 + 2.19 Re(1-\phi)^{-0.65} \quad (d \text{ to } c) \quad (27)$$

$$Sh_{oc} = -5.19 + 5.39 Re^{0.78} (1-\phi)^{-0.46} \quad (c \text{ to } d)$$

The experimental data are compared with the calculated results from the above equations in Fig. 7. This figure indicates that the suggested equation can estimate the overall continuous phase Sherwood number with high accuracy. These correlations predict the results with a reduced average error of 3.75%.

## CONCLUSIONS

(1) The experimental findings show that the mass transfer performance is strongly dependent on rotor speed and interfacial tension. Improved column performance is observed for the system of lower interfacial tension.

(2) The results show that the continuous phase velocity has little influenced on the value of  $K_{oc,a}$ , while  $K_{oc,a}$  increases with an increase in dispersed phase velocity.

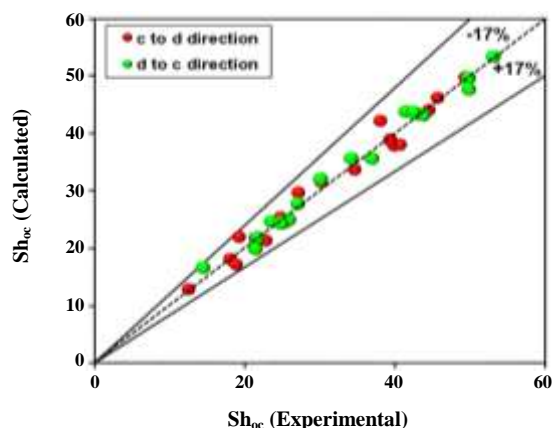


Fig. 7: Comparison between experimental data and the estimated values using equation (27).

(3) Continuous phase overall mass transfer coefficients are predicted using new correlations which is developed in this study. The proposed correlations can be applied to determine the extraction column height for various extraction processes.

(4) These correlations can be used to calculate the column height for different extraction processes. the present study is of use to those desiring to use kühni extraction column.

## NOMENCLATURE

$a$	Interfacial area, $m^2/m^3$
$B_n$	$n^{\text{th}}$ coefficient in equations
$d_{32}$	Sauter mean drop diameter, m
$D_c$	Column diameter, m
$D_R$	Rotor diameter, m
$D$	Molecular diffusivity, $m^2/s$
$E$	Axial mixing coefficient, $m^2/s$
$g$	Acceleration due to gravity, $m/s^2$
$H$	Effective height of the column, m
$K$	Overall mass transfer coefficient, m/s
$N$	Rotor speed, $s^{-1}$
$N_{ox}$	Number of 'true' transfer unit
$P$	Péclet number= $HV/E$
$Pe_c$	Continuous-phase Péclet number = $d_{32}V_s/D_c$
$Q$	Flow rate of the continuous or dispersed phase, $[m^3/s]$
$Re$	Reynolds number = $d_{32}V_s\rho_c/\mu_c$
$Sc$	Schmidt number = $\mu/(\rho D)$
$Sh$	Sherwood number = $kd_{32}/D$
$Sh_{oc}$	Overall continuous-phase Sherwood number = $K_{oc}d_{32}/D$

$t$	Time, s
$V$	Superficial velocity, m/s
$V_s$	Slip velocity, m/s
$V_t$	Terminal velocity, m/s
$x$	Mass fraction of acetone in continuous phase
$x^*$	Equilibrium mass fraction
$y$	Mass fraction of acetone in dispersed phase

## Greek Letters

$\lambda_n$	$n^{\text{th}}$ coefficient in equations (24 and 25)
$\rho$	Density, $kg/m^3$
$\Delta\rho$	Density difference between phases, $kg/m^3$
$\kappa$	Viscosity ratio ( $\mu_d/\mu_c$ )
$\sigma$	Interfacial tension
$\mu$	Viscosity
$\phi$	Dispersed phase holdup
$\psi$	Power dissipated per unit mass

## Subscripts

$c$	Continuous phase
$d$	Dispersed phase
$o$	Overall value
$x$	x-phase (continuous phase in present case)
$y$	y-phase (dispersed phase in present case)

## Superscripts

*	Equilibrium value
°	Inlet to column

Received : Jun. 28, 2016 ; Accepted : Jan. 9, 2017

## REFERENCES

- [1] Kislik V.S., "Solvent Extraction: Classical and Novel Approaches", Elsevier, New York (2012).
- [2] Aguilar M., Cortina J.L., "Solvent extraction and liquid membranes", CRC Press, New York (2013).
- [3] Jaradat M., Attarakih M., Bart H.J., Population Balance Modeling of Pulsed (Packed and Sieve-Plate) Extraction Columns: Coupled Hydrodynamic and Mass Transfer, *Ind. Eng. Chem. Res.*, **50**: 14121-14135 (2011).
- [4] Asadollahzadeh M., Torab-Mostaedi M., Shahhosseini Sh., Ghaemi A., Experimental Investigation of Dispersed Phase Holdup and Flooding Characteristics in a Multistage Column Extractor, *Chem. Eng. Res. Des.*, **105**: 177-187 (2016).

- [5] Torkaman R., Asadollahzadeh M., Torab-Mostaedi M., Determination of Slip and Characteristic Velocities in Reactive Extraction with Experiments in the Oldshue-Rushton Column and Presence of Samarium and Gadolinium Metals, *Chem. Eng. Process*, **111**: 7-13 (2017).
- [6] Asadollahzadeh M., Torab-Mostaedi M., Shahhosseini Sh. Ghaemi A., Holdup, Characteristic Velocity and Slip Velocity between Two Phases in a Multi-Impeller Column for High/Medium/Low Interfacial Tension Systems, *Chem. Eng. Process*, **100**: 65-78 (2016).
- [7] Godfrey J.C., Slater M.J., "Liquid-Liquid Extraction Equipment", Wiley, New York (1994).
- [8] Thornton J. D., "Science and Practice of Liquid-Liquid Extraction", Oxford University Press, Oxford (1992).
- [9] Ghorbanian S.A., Abolghasemi H., Radpour S.R., Modelling of Mean Drop Size in a Extraction Spray Column and Developing a New Model, *Iran. J. Chem. Chem. Eng. (IJCCE)*, **30**: 89-96 (2011).
- [10] Yuan S., Jin S., Chen Z., Yuan Y., Yin H., An Improved Correlation of the Mean Drop Size in a Modified Scheibel Extraction Column, *Chem. Eng. Technol.*, **37**: 2165-2174 (2014).
- [11] Ritcey G.M., Ashbrook A.W., "Solvent Extraction: Principles and Applications to Process Metallurgy", Elsevier, New York (1984).
- [12] Abolghasemi H., Moosavian M.A., Radpour S.R., The Effects of a Surfactant Concentration on the Mass Transfer in a Mixer-Settler Extractor, *Iran. J. Chem. Chem. Eng. (IJCCE)*, **25**: 9-15 (2006).
- [13] Li N.N., Ziegler E.N., Effect of Axial Mixing on Mass Transfer in Extraction Columns, *Ind. Eng. Chem.*, **59**: 30-36 (1967).
- [14] Bart H.G., Drumm C., Attarakih M.M., Process Intensification with Reactive Extraction Columns, *Chem. Eng. Process*, **47**: 57-65 (2008).
- [15] Henton J.E., Cavers S.D., Continuous-Phase Axial Dispersion in Liquid-Liquid Spray Towers, *Ind. Eng. Chem. Fund.*, **9**: 384-392 (1970).
- [16] Geankoplis C.J., Sapp J.B., Arnold F.C., Marroquin G., Axial Dispersion Coefficients of the Continuous Phase in Liquid-Liquid Spray Towers, *Ind. Eng. Chem. Fund.*, **21**: 306-311 (1982).
- [17] Nosratinia F., Omidkhah M.R., Bastani D., Saifkordi A.A., Investigation of Mass Transfer Coefficient under Jetting Conditions in a Liquid-Liquid Extraction System, *Iran. J. Chem. Chem. Eng. (IJCCE)*, **29**: 1-12 (2010).
- [18] Hafez M.M., Baird M.H.I., Nirdosh I., Flooding and Axial Dispersion in Reciprocating Plate Extraction Column, *Can. J. Chem. Eng.*, **57**: 150-158 (1979).
- [19] Parthasarathy P., Sriniketan G., Srinivas N.S., Varma Y.B.G., Axial Mixing of Continuous Phase in Reciprocating Plate Columns, *Chem. Eng. Sci.*, **39**: 987-995 (1984).
- [20] Kumar A., Hartland S., Prediction of Continuous-Phase Axial Mixing Coefficients in Pulsed Perforated-Plate Extraction Columns, *Ind. Eng. Chem. Res.*, **28**: 1507-1513 (1989).
- [21] Moghadam E.H., Bahmanyar H., Heshmatifar F., Kasaie M., Ziaei-Azad H., The Investigation of Mass Transfer Coefficients in a Pulsed Regular Packed Column Applying SiO<sub>2</sub> Nanoparticles, *Sep. Purif. Technol.*, **176**: 15-22 (2017).
- [22] Mišek T., Berger R., Schroter J., "Standard Test Systems for Liquid Extraction Studies", EFCE Publ. Ser. (1985).
- [23] Kumar A., Hartland S., Prediction of Axial Mixing Coefficients in Rotating Disc and Asymmetric Rotating Disc Extraction Columns, *Can. J. Chem. Eng.*, **70**: 77-87 (1992).
- [24] Skelland A.H.P., "Diffusional Mass Transfer", Wiley, New York (1974).
- [25] Lochiel A.C., Calderbank P.H., Mass Transfer in the Continuous Phase Around Axisymmetric Bodies of Revolution, *Chem. Eng. Sci.*, **19**: 471-484 (1964).
- [26] Brauer H., "Stoffaustausch Einschliesslich Chemischer Reaktionen", Verlag Sauerlander, Aarau, Switzerland (1971).
- [27] Clift R., Grace J.R., Weber M.E., "Bubbles, Drops and Particles", Academic Press, New York (1978).
- [28] Garner F.H., Foord A., Tayeban M., Mass Transfer From Circulating Drops, *J. Appl. Chem.*, **9**: 315-323 (1959).
- [29] Weber M.E., Mass Transfer From Spherical Drops at High Reynolds Numbers, *Ind. Eng. Chem. Fundam.*, **14**: 365-366 (1975).

- [30] Steiner L., [Mass-Transfer Rates From Single Drops and Drop Swarms](#), *Chem. Eng. Sci.*, **41**: 1979-1986 (1986).
- [31] Kumar A., Hartland S., [Correlations for Prediction of Mass Transfer Coefficients in Single Drop Systems and Liquid-Liquid Extraction Columns](#), *Chem. Eng. Res. Des.*, **77**: 372-384 (1999).
- [32] Torab-Mostaedi M., Safdari S.J., Moosavian M.A., Maragheh M.G., [Mass Transfer Coefficients in a Hanson Mixer-Settler Extraction Column](#), *Braz. J. Chem. Eng.*, **25**: 473-481 (2008).
- [33] Torab-Mostaedi M., Safdari J., [Mass Transfer Coefficients in a Pulsed Packed Extraction Column](#), *Chem. Eng. Process*, **48**: 1321-1326 (2009).
- [34] Torab-Mostaedi M., Jalilvand H., Outokesh M., [Dispersed Phase Holdup in a Pulsed Disc and Doughnut Extraction Column](#), *Braz. J. Chem. Eng.*, **28**: 313-323 (2011).
- [35] Torab-Mostaedi M., Asadollahzadeh M., [Mass Transfer Performance in an Asymmetric Rotating Disc Contactor](#), *Chem. Eng. Res. Des.*, **94**: 90-97 (2015).
- [36] H. Grober, Die Erwärmung und Abkühlung einfacher Geometrischer Körper, *Z. Ver. Dtsch. Ing.*, **69**: 705-711 (1925).
- [37] Kronig R., Brink J.C., [On the Theory of Extraction From Falling Drops](#), *Appl. Sci. Res.*, **2**: 142-154 (1950).
- [38] Handlos A.E., Baron T., [Mass and Heat Transfer From Drops in Liquid-Liquid Extraction](#), *AIChE J.*, **3**: 127-136 (1957).